A Compliant Multi-module Robot for Climbing Big Step-like Obstacles

S. Avinash[1], A. Srivastava[2], A. Purohit[1], S. V. Shah[1], K. Madhava Krishna[1]

***Abstract*— A novel compliant robot is proposed for traversing on unstructured terrains. The robot has a set of modules where each module contains a trunk or link and an active wheel-pair, and it is connected to the adjacent module using a passive joint. This type of robots are inherently lightweight and provide high durability due to the absence of actuators at the link joints. However, they have limited climbing ability due to tendency of tipping over while climbing big obstacles. In order to overcome this disadvantage, the use of compliant joints is proposed in this work. Spring stiffness of each compliant joint is estimated by formulating an optimization problem using the static equilibrium equations of the robot. This is one of the key novelties of the proposed work. A design methodology is also proposed for developing an n-module compliant robot for climbing given height on a surface with prescribed coefficient of friction. The efficacy of the proposed formulation is illustrated for climbing big obstacles and traversing uneven terrains using simulation of 3- and 5-module robots. The robot is successfully able to climb maximum heights of 17 cm and 36 cm using 3 and 5 modules, respectively. Mechanical and electrical design of the robot is conceived, and a working prototype of the robot is developed. Simulation results are validated using the prototype.**

I. Introduction

The aim of this paper is to propose a compliant modular robot which has enhanced step climbing ability with open-loop operation. This is one of the key functional capabilities desired in urban search and rescue(USAR) [1] and planetary exploration missions. The use of robots in such scenarios is well documented [2], [3], [4]. Specifically, urban environments predominantly consist of structured obstacles like steps, stairs, curbs, etc. A robot that can successfully navigate over these obstacles could help in creating many potential applications for robots in urban environments.

An alternative type of robots, comprising of multiple modules have also been reported [5]. Unlike the above-mentioned wheeled mobile robots, the functionality of multi-module robots can be improved by adding modules [6].

Modular Robots have been proposed and successfully used in USAR scenarios [5]. The have additional functionality that make them a better choice [6]. Modular robots have low ground clearance and the ability to naturally deform along the obstacles on an uneven terrain. However, their ability to climb big step-like obstacles is seldom reported. This work presents a novel modular wheeled robot for climbing big-step like obstacles in an open-loop condition. The prototype of the robot is shown in Fig. 1. The proposed robot comprises of 3 modules where each module has a trunk/link with an active wheel-pair connected to it. The adjacent modules are connected by passive joints. Such robots have been categorized in literature as Active-Wheel Passive-Joint (AW-PJ) robots [7]. Snake-like robots such as Genbu [8] belong to this category. Several types of snake-like robots have been proposed earlier in the literature. They are broadly classified into crawler-type or wheel-type based on the type of locomotion mechanism. They can also be classified based on the mode of actuation used for their locomotion, i.e., active-wheel/active-crawler (AW/AC) and/or active-trunk-joint (AJ). Table I depicts this classification. AW-PJ type robots typically suffer from the problem of modules tipping over while climbing big step like obstacles. In this work, the use of compliant joints is proposed in order to safeguard the robot from tipping over while climbing heights which are more than its link length.

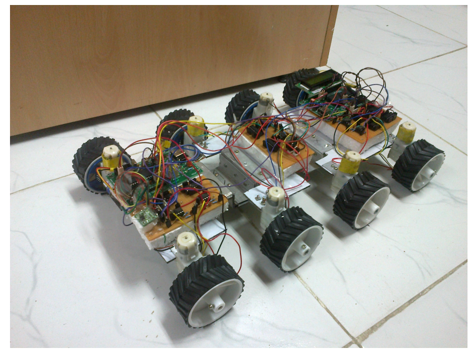

Fig. 1. A snapshot of the 3-module complaint robot prototype.

While crawler robots have better climbing ability than wheel robots, the former are slower, bulkier. Therefore, the proposed robot uses wheels for their 1) simplicity in design, 2) speed and 3) ability to provide sufficient ground clearance. It consists of three modules connected by passive trunk-joints and active wheels, thus belonging to the AW-PJ (active-wheel passive-trunk-joint) category. The use of active-trunk-joints for step climbing was shown in [13] using modular robot. In [14], [8] the authors have shown that the robots

TABLE I

Classification of snake-like robots

Existing Robots	Locomotion Mechanism	Trunk Actuation	Robot Category
ACM -R4 [9]	Wheel	Active	AW-AJ
Genbu [8]	Wheel	Passive	AW-PJ
ACM-R3 [7]	Wheel	Active	PW-AJ
Shouryu III,IV,V [10], [11]	Crawler	Active	AC-AJ
Kohga [12]	Crawler	Passive	AC-PJ

*This work is not supported by any organization. All authors are with the Robotics Research Lab, IIIT-Hyderabad, India

with active-trunk-joints are more prone joint-motor/gear-train damage when subjected to high reaction forces/moments due to impact. On the other hand, snake-like robots with passive trunk-joints are more durable as the joints can freely deform along the terrain. However, they can tip-over while climbing high step-like obstacles.

It is seen that the use of compliant joints improves the climbing efficiency of the robot by maintaining wheel ground contact, and the redistribution of normal forces for generating traction efficiently. The determination of stiffness at the compliant joints is formulated as an optimization problem with an objective to generate minimal spring reaction moments while climbing. This is one of the main contributions of this work. Motivated by the development of this modular robot, a design methodology is also proposed for developing an n-module compliant robot for climbing a given height h on a surface whose coefficient of friction is μ. The successful validation of the methodology in developing a five module robot for climbing a step of 36cm height is also shown.

The rest of the paper is organized as follows: Section II introduces a modular robot mechanism and discusses the issues with passive trunk-joint robots. Section III presents an optimization formulation for designing compliant joints for the modular robot. In Section IV, a design methodology is proposed for developing an n-module compliant robot. The simulation results, overview of the working prototype, and its experimental validation are provided in Section V. Finally, conclusions and future work are given in Section VI.

II. Model Description

As described in the previous section the proposed robot belongs to AW-PJ class were the active wheels help in propulsion, and the passive trunk-joints aid in freely deforming along the terrain. The proposed robot has 3-modules, each consisting of an independently actuated wheel-pair and a trunk/link. Two adjoining modules are connected using 1 degree-of-freedom (DOF) revolute joints, called trunk-joints. The wheel- and trunk-joints are denoted by W_i and J_i, respectively, as shown in Fig. 2. The absolute (between module i and ground) and relative (between module i and $i{+}1$) trunk joint angles are denoted by θ_i and ϕ_i, respectively, as shown in Fig. 2. Minimum ground clearance and link joint placement are important design considerations. They are discussed in sufficient detail in (addref).

The Specifications of the proposed robot are listed in Table II. Upon finalizing the robot's design, its climbing ability with passive trunk-joint is analyzed next.

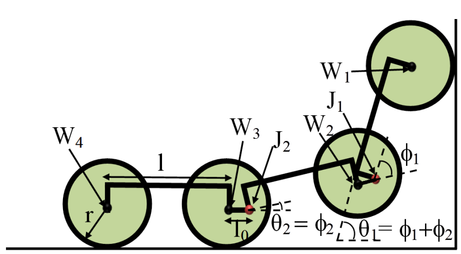

Fig. 2. The front view of the robot showing the trunk and wheel joints. The relative angles (ϕ's) and absolute angles (θ's) are also depicted.

TABLE II
SPECIFICATIONS OF THE 3-MODULE ROBOT

Symbols	Quantity	Values(with Units)
l	Link Length	0.15 m
b	Link Breadth	0.1 m
r	Wheel Radius	0.03 m
l_0	Wheel Joint and Link Joint Offset	0.03 m
μ	Coefficient of Friction	0.8
τ_{wmax}	Stall Torque of Wheel Motors	0.6 Nm
m_w	Mass of Each Wheel	0.1 Kg
m_l	Mass of Each Link	0.3 Kg

A. Climbing Analysis with Passive Trunk-Joint

Fig. 3(a) shows the climbing phase of the robot with passive trunk-joint. Note that module 1 will continue to climb along the step till it crosses a limiting angle. Beyond the limiting angle the module will tip-over as shown in Fig. 3(b). The limiting angle called tip-over angle (θ_{to}) can be determined based on the position of center-of-mass (COM) of the module as $\theta_{to} = \pi/2 - tan^{-1}(y_{COM}/x_{COM})$, where x_{COM} and y_{COM} denote the COM coordinates of the module. This tip-over phenomenon limits the climbing ability of the proposed robot, and the robot can only climb obstacles of heights less than or equal to $lsin(\theta_{to})$.

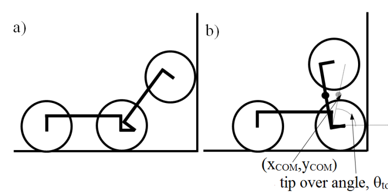

Fig. 3. Climbing behavior of the passive robot

This work mainly aims to improve the climbing ability of a passive multi-module robot. In order to overcome the problem of tip over, we propose the use of compliant joints consisting of torsional springs. This is one of the fundamental contributions of this work. It will be shown that the use of springs also helps in increasing the wheel traction by shifting the normal force towards wheel-pair in every module. These effects will be studied in sufficient detail in the next section.

III. Stiffness Estimation and Design Validation

The stiffness of a compliant joint plays a key role in the overall performance of the robot. For the robot shown in Fig. 2, designing J_1 with high stiffness causes the wheel-pair at W_2 to lift off the ground early. This results into reduction in the push force required for climbing. On the other hand, use of joint with low stiffness at J_1 may not be able to resist moment causing tip over. Therefore, an optimal value for stiffness has to be determined such that the wheel-pair lift off the ground as late as possible, and tip over is avoided. Therefore, stiffness estimation is formulated as an optimization problem with the objective to minimize moments at the joints J_1 and J_2 while climbing. Note that the dynamical effects are neglected as the robot moves with low velocities during climbing phase.

A. Optimization Formulation

Tip over can be avoided if the moments generated by springs can balance the net moment generated at the joints. For this, climbing maneuver from $h = 0$ to $2lsin\theta_{to}$ is discretized into p set points, and the moment profiles for joints J_1 and J_2 are obtained using the static stability equations. It may be noted that, the traction and normal forces, at the wheel-ground interface, appearing in the static stability equations are difficult to determine accurately without direct sensing. Therefore in the numerical model, they are generally assumed to be unknowns and the static stability equations are under-determined [15]. Though, a least norm solution can be obtained, it may not be of physical significance. Hence, calculation of moments at the joints, and traction and normal forces are formulated as an optimization problem. The objective function for the optimization is taken as minimization of the joint moments. The above equation ensures that the spring required to balance the net joint moment is not very stiff. The objective function is given below:

$$\underset{\mathbf{D}}{\text{minimize}} \quad \sum_{j=1}^{p} \boldsymbol{\tau}^j \qquad \text{subject to} \quad \mathbf{F} \leq \mu \mathbf{N}, \qquad (1)$$

where, $\boldsymbol{\tau} = [\tau_1 \;\; \tau_2]^T$, $\mathbf{F} = [F_1 \;\; F_2 \;\; F_3 \;\; F_4]^T$, $\mathbf{N} = [N_1 \;\; N_2 \;\; N_3 \;\; N_4]^T$, and the vector of design variable $\mathbf{D} = [\mathbf{F}^T \; \mathbf{N}^T \; \boldsymbol{\tau}^T]^T$. Moreover, F_i's and N_i's denote traction and normal forces acting at wheel-pair i, and τ_i's denote the moments at the link joints. Note that the traction forces are constrained by the maximum torque (τ_{wmax}) of the wheel motors as $F \leq \tau_{wmax}/r$. The system is also constrained by the static stability equations of the robot, which are derived in the next subsection.

B. Quasi Static Model for the Compliant Robot

Since the robot is symmetric about the sagittal plane, a planar quasi-static analysis of the robot can approximate its real behavior. This, however, is non trivial for multi-module robot discussed in this paper. In mobile robots, like, CRAB [16] and PAW [15], the wheels maintain contact with the ground throughout their motion. This enables the formulation of a generalized set of equations for any arbitrary configuration. However, here, the static stability equations change when wheel-pair leaves contact with the ground during the climbing phase of the robot. Therefore, different set of equations have to considered for various configurations of the robot while optimization. In the first phase, the robot climbs heights up to $lsin\theta_{to}$ using only one link, whereas it climbs from $lsin\theta_{to}$ to $2lsin\theta_{to}$ in the next phase with two links. Figures 4(a) and 4(b) show the two climbing phases for a 3-module robot. It also depicts the forces and moments acting on it. Equations for Phase-1 are given in (1). Similar set of equations can be obtained for Phase-2 by substituting

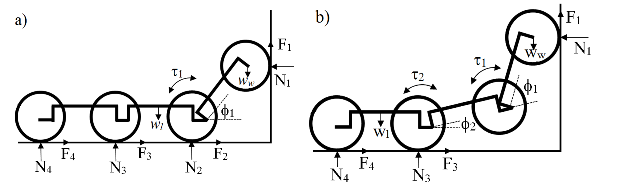

Fig. 4. Depiction of static forces and moments acting on the robot: The forces and moments are shown for the two possible climbing configurations ie., a) Phase-1: when only one module is climbing and b)Phase-2: when two modules are climbing

$F_2 = N_2 = 0$, denoting a loss of contact for the second wheel-pair.

$$\begin{aligned}
& && \textit{One module climbing} \\
&\sum F_x = 0 && N_1 - F_2 - F_3 - F_4 = 0 \\
&\sum F_y = 0 && 3w_l + 8w_w - 2F_1 - 2N_2 - 2N_3 - 2N_4 = 0 \\
&\sum M_{J_1} = 0 && 2F_1 r + 2F_1 lcos\theta_1 + 2N_1 lsin\theta_1 - \\
& && 2w_w lcos\theta_1 - w_l[(l/2)cos\theta_1 - csin\theta_1] \\
& && -\tau_1 = 0 \\
&\sum M_{J_2} = 0 && 2F_2 r + N_2 l - 2w_w l - w_l(l/2) - \\
& && [(2w_w + w_l) - 2F_1](l + l_0) + \tau_1 \\
& && -\tau_2 = 0 \\
&\sum M_{W_4} = 0 && 2F_3 r + 2F_4 r + 2N_3 l - 2w_w l - w_l(l/2) - \\
& && [2(2w_w + w_l) - 2F_1 - 2N_2](l + l_0) \\
& && +\tau_2 = 0
\end{aligned}$$

where τ_{wi} is the i_{th} wheel torque, w_l and w_w are the weights of the link ($m_l g$) and wheel-pair ($m_w g$), respectively. For Phase-1, $\phi_1 = \theta_1 = sin^{-1}(h/l)$ and $\phi_2 = 0$, and for Phase-2, $\phi_2 = \theta_2 = sin^{-1}(h - lsin\theta to)/l)$ and $\phi_1 = \theta_{to} - \phi_2$. Here, the second module will begin to climb only after the first module reaches $lsin\theta_{to}$. In Phase-2, ϕ_1 is designed such that if ϕ_2 increases ϕ_1 decreases by the same amount maintaining $\theta_1 = \theta_{to}$, in order to avoid tipping over.

C. Estimation of stiffness

The profile of joint moments ($\boldsymbol{\tau}$) versus joint angles ($\boldsymbol{\phi} = [\phi_1 \;\; \phi_2]^T$) obtained from the above optimization is shown in Fig. 5 with a solid curve. The profile is slightly non-linear as evident from the figure. Hence, a least squares approximation is carried out as

$$\underset{\mathbf{k}}{\text{minimize}} \quad \sum_{j=1}^{p} (\boldsymbol{\tau}^j - \mathbf{k}\boldsymbol{\phi}^j)^2 \quad , \qquad (2)$$

where $\mathbf{k} = diag(k_1, k_2)$ and k is the stiffness of the i^{th} joint. The least squares fit for both the joints is also shown in Fig. 5 by dotted lines. Values of k_1 is determined as $0.0105N - m/deg$ while k_2 is of order 10^{-6}, and hence, it is assumed to be zero.

According to the results obtained from the above optimization procedure, a compliant joint was developed at J_1.

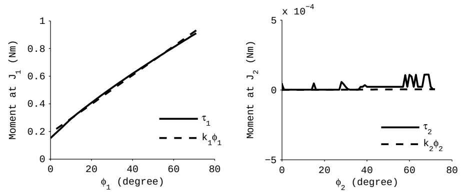

Fig. 5. Moment plots for joints J_1 and J_2: The plot shows the desired moments obtained from the optimization procedure (solid line) and the moments generated by the optimal spring (dotted line). The slope of the the dotted line yields the spring stiffness value

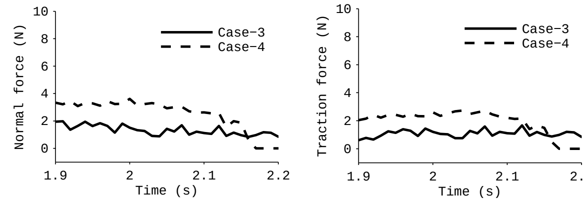

Fig. 8. Utility of spring at J_2 while climbing a step of 16cm: Plots showing the variation Normal and Traction forces at wheel 2 with spring (Case-4) and without spring(Case-3) at J_2.

It is also desired that the springs only act against counter-clockwise moments and don't resist any clockwise moments. This helps in freely deforming on an uneven terrain without any resistance when there is no scope for tipping over. Hence, the spring is fitted to module 2 and it only touches module 1 without any permanent connection. This enables the springs to act only when there is a positive angular displacement between the two modules.

D. Design Validation

Four different step climbing experiments were carried out to show the efficacy of the compliant joints in improving the climbing ability of a the robot. Each row in Fig. 6 shows the snapshots of a different experiment. In Case-1 (Fig. 6(a)-(c)), the robot consisting of joints without springs failed to climb a step of height 14cm. On the other hand, the same robot (Case-2), with a spring at J_1, was able to successfully climb over the step, as shown in Fig. 6(d)-(f). Figure 7(a) shows the plot of joint angles ϕ_1 for the above two cases. In Case-1, the absolute angle increased indefinitely and resulted in tip over, whereas in the second case the angle rose till $68^0 (\approx \theta_{to})$ and then decreased as it successfully climbed the step. The use of compliant joint in Case-2 increased the normal force, N_1, at wheel-1 facilitating the wheels to apply more traction (F_1) and thus successfully climbed without slipping, as shown in Fig. 7(b). Interestingly, in Case-1 wheel-1 lost contact with the wall multiple times. This is due to the fact that the normal force became zero several times, as shown in Fig. 7(b). While in Case-2, the wheel never lost contact with the step, i.e., $N_1 > 0$. This advantage confirms the superiority of the compliant joint over mechanical lock. Additionally, the slip rate was found to be more bounded in Case-2 than that of Case-1 as depicted in Fig. 7(c).

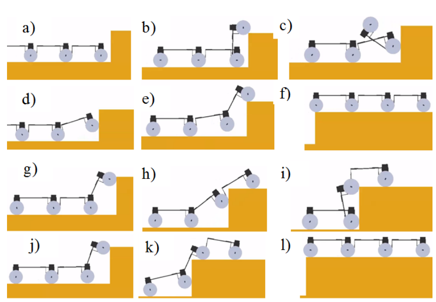

Fig. 6. Step climbing ability of the 3-module robot: a)-c) Case-1: the passive robot tips over while climbing a height of 14 cm; d)-f) Case-1: it successfully climbs the step of 14 cm using a compliant joint at J_1; Case-3: g)-i) the robot with a compliant joint at J_1 manages to climb a height of 16 cm but is unable to pull the remaining links; Case-4: j)-l) it is able to fully climb a height of 16 cm using compliant joints at J_1 and J_2

In Case-3 (Figs. 6(g)-(i)), the robot with only compliant joint at J_1 was made to climb a step of height 16 cm. The robot was able to climb height of 16 cm against the wall but failed to pull up the remaining modules due to the lack of push force as illustrated in Fig. 6(i). Note that the optimization only takes into consideration the climbing phase of the robot, hence, it may happen that the robot may climb height h but not have enough pulling force to lift remaining modules. In other words, the traction force F_2 reaches the limiting case μN_2 thus not allowing the wheel to apply greater traction to climb the step, as depicted in Fig. 8 with solid lines. However, this limitation can be overcome using another compliant joint at J_2 having the same stiffness value as that of J_1. In case-4 (Figs. 6(j)-(l)), the robot with two compliant joints successfully climbed a step of 16cm height. Here, the normal force at wheel-2 increased, and this allowed it to apply greater traction force, as shown in Fig. 8 with dotted lines.

IV. Height Climbing Ability of an n-Module Compliant Robot

A general methodology has been developed for estimating the maximum height climbing ability of an n-module compliant robot. This height climbing ability depends chiefly on the coefficient of friction μ and the maximum wheel torque τ_{wmax}. For a practical modular robot design, the quasi-static analysis based optimization formulation can be used to determine the maximum height, h_{max}. To this end, firstly, a trajectory for tip-over-free step climbing is generated for some large height value. It is then discretized into p set-points and the joint angles ϕ_i for all the set-points are derived. They are then used to obtain the static stability equations. Note that, an n-module robot has $n+1$ wheel-pairs and during the climbing maneuver, one-by-one, n wheel-pairs may lift off the ground to successfully climb without tipping over. As each wheel-pair lifts off the ground, the static-stability equations for the system change. To reflect the same, the climbing process of the robot is divided in to n phases, where each phase uses one set of static stability equations.

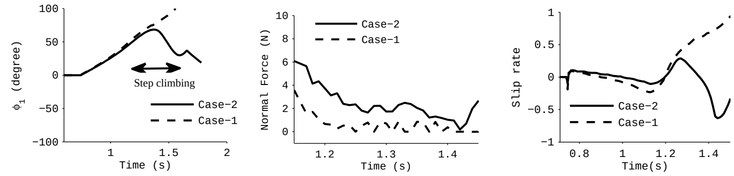

Fig. 7. Plots to analyze robot's climbing behavior while climbing a 14cm step: a)-c) The comparison of the joint angle (ϕ_1), normal force(N_1) and slip rate(at Wheel 1) between cases with spring (Case-2) and without spring (Case-1) at J_1

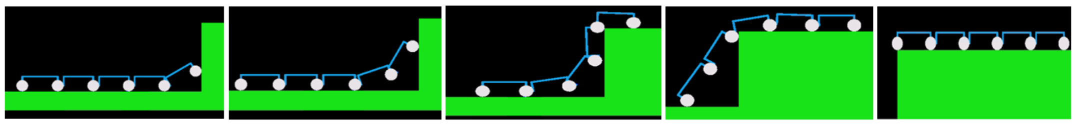

Fig. 9. A 5 module compliant robot with compliant joints at J_1 and J_2 climbs a height of 36cm

A. *Determination of the Joint Trajectories*

$$h = \sum_{i=1}^{n} l sin\theta_i \quad where, \quad \theta_i = \sum_{i=1}^{n} \phi_i \quad \forall i \in n \tag{3}$$

$$\begin{aligned} &\phi_s = sin^{-1}(h - (s-1) l sin\theta_{to}/l) \\ &\phi_{s-1} = \theta_{to} - \phi_s \\ &\phi_i = 0 \quad \forall i \in n \backslash \{s, s-1\} \end{aligned} \tag{4}$$

$$\begin{aligned}
&\sum F_x = 0 && N_1 - \sum_{i=s+1}^{n} F_i = 0 \\
&\sum F_y = 0 && 2(n+1)w_w + n w_l - 2F_1 - \sum_{i=s+1}^{n} N_i = 0 \\
&\sum M_{J_1} = 0 && 2F_1 r + (2F_1 - 2w_w) l cos\theta_1 \\
& && - w_l[(l/2)cos\theta_1 - c sin\theta_1] \\
& && + 2N_1 l sin\theta_1 - \tau_1 = 0 \\
&\sum M_{J_j} = 0 && \tau_{j-1} - \tau_j - w_l[(l/2)cos\theta_j - c sin\theta_j] + \\
&\forall j \in \{2, s\} && [(j-1)(w_l + 2w_w) - 2F_1)(l + l0)cos\theta_j \\
& && + 2N_1 l sin\theta_j = 0 \\
&\sum M_{J_q} = 0 && 2F_q r + 2N_{q-1} l - 2w_w l - w_l(l/2) - \\
&\forall q \in \{n \backslash s\} && [(s+q-1)(2w_w + w_l)](l + l0) - \\
& && (2F_1 + 2\sum_{t=1}^{q-1} N_t)(l + l_0) + \tau_{q-1} - \tau_q = 0 \\
&\sum M_{W_{n+1}} = 0 && 2F_{n+1} r + 2F_n r + 2N_{n-1} l - \\
& && [2(2w_w + w_l) - 2F_1 - 2\sum_{t=s+1}^{n} N_t](l + l_0) \\
& && - 2w_w l - w_l(l/2) + \tau_{n-1} = 0
\end{aligned} \tag{5}$$

Designing the joint trajectories for an n-module robot can be a challenging task. For this, a trajectory is developed first for the COM of the first wheel-pair and the corresponding joint motions are derived next. Trajectory of the first wheel-pair ideally follows the profile of a step or obstacle. For climbing the step, as shown in Fig. 6, trajectory of the first wheel can be assumed to be a straight line of a large length value. Next, the trajectory is discretized into p set-points and the desired joints angles (ϕ_i's) are then determined at each set-point. It is ensured that the absolute angles θ_i's of all the climbing links lie under θ_{to}, to avoid tip over. This can be achieved by progressively increasing the relative angle (ϕ_{i+1}) at the succeeding joint and decreasing that of the preceding joint (ϕ_i), as the height keeps on increasing. This is the key idea used for climbing any height h using an n-module compliant robot without tipping over. The joint angles ϕ_i for different set-points can be obtained by solving the set of equations given in (3). The procedure for solving the above equations for Phases-1 and -2 have been shown in the previous section. A generalized form of the same is given in (4), to calculate the ϕ_i's for any set point in Phase-s. The joint trajectories thus obtained are used to evaluate the static stability equations of the n-module robot as shown in (5)

B. *Estimation of h_{max} and $\mathbf{k}$*

Section III describes in sufficient detail how the quasi-static analysis is performed for a 3-module robot. The same can be extended for an n-module robot. The number of quasi-static equations' sets are equal to the number of climbing phases s wherein the static-stability equations are satisfied for a given n-module robot. It can be noted that $s \in \{1, n\}$. The generalized quasi-static equations for an n-modular robot in Phase-s are given in (5). The equations are evaluated at each intermediate height. The optimization procedure is carried out for all the set points until the quasi-static constraints are violated. This determines the maximum height, h_{max}, that the robot can climb without tipping over. Thereafter, the desired moments($\boldsymbol{\tau}$) that are obtained from the optimization procedure are least squares approximated to determine the stiffness values($\mathbf{k}$) for their respective joints.

V. Results and Discussions

Extensive simulations were carried out to demonstrate the effectiveness of compliant joints in avoiding tip over and improving the robot's step climbing ability. The results are already reported in Section-III. Figures 6, 7 and 8 show

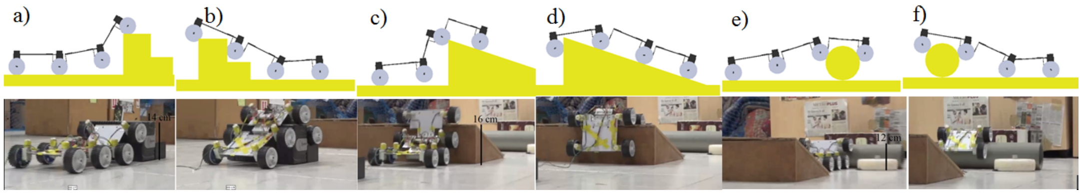

Fig. 10. Demonstrating the climbing ability of the 3-module robot in simulation (top row) and experiment (bottom row): In a)-b), the obstacle is a rectangular block of 14 cm height; In c)-d), it is wooden ramp of maximum height 16 cm; Finally, in c)-d), the obstacle is a cylindrical pipe of 12 cm diameter

that, the use of springs has not only helped in avoiding tip-over but it also increased the normal force at the climbing wheel-pair's contact and enabled it to generate more traction without slipping. In order to validate the simulation results, an experimental prototype of a compliant robot was developed. Its climbing ability was assessed on different types of obstacles, first numerically, and then experimentally.

The climbing ability of the robot with compliant joints was tested on an uneven terrain created using obstacles made of different materials and of varying heights, as shown in Fig. 10. It was observed that the climbing ability of the robot improved remarkably with the addition of springs. The terrain consisted of a rectangular block of 14 cm height, a ramp of maximum height 16 cm and a cylindrical pipe of 12 cm diameter. The robot was able to successfully climb over all these obstacles. This validates the effectiveness of the proposed design of compliant robot.

VI. Conclusions and Future Work

This work presents a methodology for designing a modular compliant robot to climb big step-like obstacles and traverse on a highly uneven terrain. The methodology is used to determine the spring stiffness values for the compliant joints by formulating an optimization problem built upon the quasi-static analysis of the robot. Using this methodology, 3- and 5-module compliant robots were successfully simulated for climbing heights upto 17mm and 36mm, respectively. An experimental prototype of the 3-module robot was also built to validate the results of simulation.

It is shown that the compliant joints not only helps in avoiding tip over, but also facilitates in maintaining contact between the step and the climbing wheel-pair, thus avoiding intermittent slip. Additionally, when a non-climbing wheel-pair leaves contact, the use of spring also helps in effective redistribution of its normal force among neighboring wheel-pairs, thus enabling them to apply greater traction and achieve successful climbing.

The major focus of the future work would be to provide semi-autonomous capabilities to the robot. To this end, controllers will be developed for safe climbing down motion, obstacle detection, etc.

Acknowledgments

The authors would like to thank Arun Kumar Singh and Anurag VV for their support during the formative stages of this project. Thanks is also due to Priya Bansal for her help during the fabrication and experimental testing of the prototype.

References

[1] Elena Messina and Adam Jacoff. Performance standards for urban search and rescue robots. In *Defense and Security Symposium*, 2006.

[2] A. Davids. Urban search and rescue robots: from tragedy to technology. *IEEE Intelligent Systems*, 2002.

[3] Erico Guizzo. Japan earthquake: Robots help search for survivors. *IEEE Spectrum*, 2011.

[4] Erico Guizzo. Japan earthquake: More robots to the rescue. *IEEE Spectrum*, 2011.

[5] Mark Yim, Wei-Min Shen, Behnam Salemi, Daniela Rus, Mark Moll, Hod Lipson, Eric Klavins, and Gregory S Chirikjian. Modular self-reconfigurable robot systems [grand challenges of robotics]. *IEEE Robotics & Automation Magazine*, 2007.

[6] David Duff, Mark Yim, and Kimon Roufas. Evolution of polybot: A modular reconfigurable robot. In *Harmonic Drive International Symposium*, 2001.

[7] Shigeo Hirose and Hiroya Yamada. Snake-like robots [tutorial]. *IEEE Robotics & Automation Magazine*, 2009.

[8] Hitoshi Kimura and Shigeo Hirose. Development of genbu: Active wheel passive joint articulated mobile robot. In *IEEE/RSJ International Conference on Intelligent Robots and Systems (IROS)*, 2002.

[9] Hiroya Yamada and Shigeo Hirose. Development of practical 3-dimensional active cord mechanism acm-r4. *Journal of Robotics and Mechatronics*, 2006.

[10] Masayuki Arai, Toshio Takayama, and Shigeo Hirose. Development of souryu-iii: connected crawler vehicle for inspection inside narrow and winding spaces. In *IEEE/RSJ International Conference on Intelligent Robots and Systems (IROS)*, 2004.

[11] Masayuki Arai, Yoshinori Tanaka, Shigeo Hirose, Hiroyuki Kuwahara, and Shingo Tsukui. Development of souryu-iv and souryu-v: serially connected crawler vehicles for in-rubble searching operations. *Journal of Field Robotics*, 2008.

[12] Tetsushi Kamegawa, Tatsuhiro Yamasaki, Hiroki Igarashi, and Fumitoshi Matsuno. Development of the snake-like rescue robot. In *IEEE International Conference on Robotics and Automation (ICRA)*, 2004.

[13] Mark Yim, Sam Homans, and Kimon Roufas. Climbing with snake-like robots. In *IFAC Workshop on Mobile Robot Technology*, 2001.

[14] Kousuke Suzuki, Atsushi Nakano, Gen Endo, and Shigeo Hirose. Development of multi-wheeled snake-like rescue robots with active elastic trunk. In *IEEE/RSJ International Conference on Intelligent Robots and Systems (IROS)*, 2012.

[15] K. Turker, I. Sharf, and M. Trentini. Step negotiation with wheel traction: a strategy for a wheel-legged robot. In *IEEE International Conference on Robotics and Automation (ICRA)*, 2012.

[16] Ambroise Krebs, Thomas Thueer, Stéphane Michaud, and Roland Siegwart. Performance optimization of all-terrain robots: a 2d quasi-static tool. In *IEEE/RSJ International Conference on Intelligent Robots and Systems (IROS)*, 2006.